12. F. P. Bretherton, R. E. Davis, C. B. Fandry, *Deep-Sea Res.* **23**, 559 (1976).
13. If the density field remains unchanged as for barotropic motions, a change in sea level of 1 cm causes a change in bottom pressure of ~1 mbar.
14. W. D. Nowlin, R. D. Pillsbury, J. Bottero, *Deep-Sea Res.* **28A**, 1 (1981).
15. Before contouring, the data were interpolated to a grid 400 km by 400 km and smoothed over adjacent grid points. The resultant rms error for the map is estimated to be less than 4 cm.
16. The correlation coefficient (sea level versus time) averaged over the 229 clusters (weighted by variance) is 0.7 ± 0.3.
17. See (*11*) for a bathymetry map.
18. The rms accuracy of the TOPEX altimeter is expected to be 14 cm [see TOPEX Science Working Group, *Satellite Altimetric Measurements of the Ocean* (Publication 400-111, Jet Propulsion Laboratory, Pasadena, 1981).
19. We thank M. Parke for useful discussions. The ISOS pressure record used in the study was provided by R. B. Wearn. This research was performed at the Jet Propulsion Laboratory, California Institute of Technology, and at Oregon State University under contract with the National Aeronautics and Space Administration.

20 April 1984; accepted 11 June 1984

Extensive Volcanism Associated with the Separation of Australia and Antarctica

Abstract. *Alternating hard and soft layers characterize the Gull Rock and Tuit Members of the late Eocene Blanche Point Formation, South Australia. Originally the formation was mainly a mixture of volcanic ash, sponge spicules, and calcareous fossil remains, with hard layers produced later by selective silicification. It resembles Cretaceous sediments from western Europe and the eastern coast of the United States, and in each case it appears that alteration of volcanic ash produced smectite and clinoptilolite with release of silica that subsequently crystallized as opal-CT. The occurrence of similar deposits from New Zealand to as far west as Albany, Western Australia, indicates extensive volcanic activity south of Australia in the late Eocene resulting from rifting and separation from Antarctica.*

The Blanche Point Formation consists of about 30 m of fine- to medium-grained sediment deposited in the St. Vincent Basin, South Australia; Reynolds (*1*) described it as a series of hard and soft marls because of the occurrence of numerous, rather regularly silicified, layers within parts of an otherwise weakly lithified claystone. The layers are not entirely coincident with rather indefinite bedding. We consider the origin of the formation as a whole and relate this to regional tectonics, namely, the separation of Australia and New Zealand from Antarctica.

Details of the lithostratigraphy are given in (*2*) and summarized in Fig. 1. Apart from the extra silica in the silicified layers, the rocks consist mainly of calcareous and siliceous fossil fragments with a substantial intermixture of clay minerals ranging in representative samples from 3 to 30 percent. The biogenic component ranges from 25 to 80 percent, quartz from 1 to 13 percent, and coarser, authigenic, generally well crystallized, clinoptilolite, and opal-CT constitute most of the rest (Fig. 2).

The clay minerals, except in the Perkana Member, are mainly smectites containing only 5 to 15 percent interlayered illite (*3*). The Perkana Member also contains kaolinite, which appears to be pseudomorphous after the smectite and formed by alteration of it. Glauconite, much of it pelletal, also occurs throughout the formation but is most abundant in the Tuketja Member. Discrete illite, which may be of detrital terrigenous origin, is minor, and originally the bulk of the clay mineral assemblage throughout the sequence was smectite.

The quartz was initially thought to be of detrital terrigenous origin (Fig. 3, A and B). Although transport in suspension could account for the lack of rounding, the general lack of mosaic texture and the sharp extinction of most grains is evidence of igneous origin. No other primary volcanic component has been recognized.

Sediments formed by diagenetic alteration of vitric ash generally contain smectite, silica minerals, and zeolites. Although the presence of any one of the minerals is not diagnostic, the occurrence of all three in the Blanche Point Formation is strongly suggestive of alteration of volcanic ash. Further, the presence of more than 90 percent essentially pure smectite in the carbonate-free fraction of a sediment of less than 2 μm in diameter appears to be generally accepted as evidence of formation of the smectite by alteration of volcanic ash (*4, 5*). Illite layers comprise less than 15 percent of the predominant smectite of the fraction of less than 2 μm from Blanche Point, supporting a volcanic origin for this component.

Much evidence, including the pristine nature of most of the sponge spicules and the results of chemical mass balance calculations, suggests that silica released by decomposition of original volcanic ash recrystallized as opal-CT. Intensive searching disclosed no evidence of the presence of diatoms or radiolaria.

We conclude that the Blanche Point Formation is of biogenic and volcanic origin, with the formation of the clay minerals and clinoptilolite and the silicification of preferred layers being the result of penecontemporaneous or subsequent diagenetic processes.

Coeval neritic sediments of similar aspect occur sporadically along the southern Australian margin between longitudes 143°30′E and 117°E. In the west, the nonterrigenous portion of the late Eocene Plantagenet Group (*6*) consists mainly of smectite or kaolinite, clinoptilolite, opal-A, and opal-CT; in the east, late Eocene clays at Browns Creek show comparable evidence of volcanic origin. An interval of interlayered tuffs, marls, and spicular marine diatomite beds occurring within the late Eocene Waiareka Volcanic Formation of southern New Zealand at the time shows a direct link between alteration of volcanic sediments and mobilization of silica.

Preservation of such potentially ephemeral neritic ash deposits must demand special conditions: a strong terrigenous input would swamp the ash;

BLANCHE POINT FORMATION	Tuit Member	Calcareous, spicular clays and silts; opal-CT layers	Foraminifera and other microfossils	Macrofossils: molluscs, nautiloids and brachiopods, thalassinoid burrows
	Perkana Member	Calcareous clayey spongolite		
	Gull Rock Member	Calcareous, spicular clays and silts; opal-CT layers		Macrofossils: molluscs and nautiloids, thalassinoid burrows
	Tuketja Member	Glauconitic, spicular clayey limestone		Macrofossils: brachiopods

Fig. 1. Stratigraphy of the Blanche Point Formation.

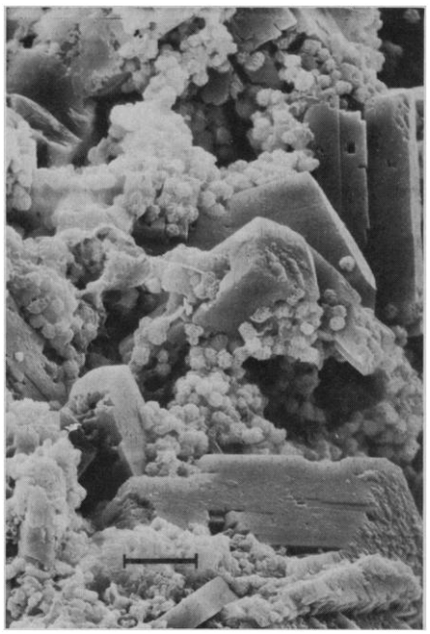

Fig. 2. Euhedral partially corroded crystals of clinoptilolite with associated opal-CT lepispheres. Scale bar, 10 μm.

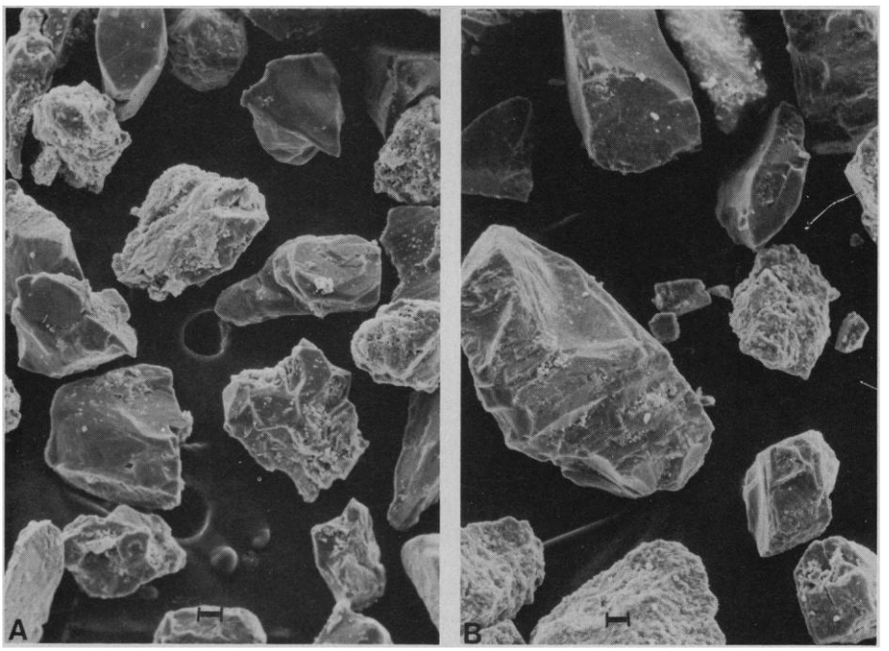

Fig. 3. (A) Sharply angular quartz grains in a separate from the Gull Rock Member, Blanche Point Formation. A few adhering opal-CT lepispheres are present on some of the grains. (B) A separate from the Wairoa Ash, New Zealand, for comparison. Scale bar, 10 μm.

strong currents would disperse it. There is paleontological evidence of restricted water circulation in the Willunga Embayment (*7*), perhaps suggesting a partially barred basin. The virtual absence of detrital terrigenous material in the Blanche Point Formation signals a striking change from the environmental conditions which prevailed during the deposition of the relatively coarse-grained fluvial and paralic sands that form the older part of the local Eocene. Well-developed cross-bedding and numerous channels in these sands suggest rapid sediment deposition, which is mirrored widely in other southern Australian Tertiary basins (*8–10*). During deposition of the Blanche Point Formation a change of facies to lignite deposits adjacent to the extreme eastern margins of the St. Vincent Basin indicate coastal swamps (*11*), which may have prevented the ingress of a much lessened fluvial load. Changes in the terrigenous regime and runoff, which led to this sharp alteration in clastic supply, pose intriguing questions, the answers to which will demand a greater understanding of the climatic conditions and history of this continental margin.

The site of the explosive volcanism that provided material for the deposition of the Blanche Point Formation is not known, but it was probably related to the separation of Australasia and Antarctica. Volcanic sediments of similar age have been reported in cores from the Deep-Sea Drilling Project (*12, 13*) between Australasia and Antarctica; all intersected glauconitic spicular sediments of late Eocene age and chert nodules, opal-CT, clinoptilolite, and volcanic smectite occur in varying proportions.

Hole 264 of the Deep-Sea Drilling Project (*12*), southwest of the Australian continent, intersected not only the late Eocene volcanic debris that appears to be the result of rifting between Australasia and Antarctica, but also Upper Cretaceous volcanoclastics presumably associated with rifting in the Indian Ocean. Intervals containing smectite, opal-A (radiolarian tests), opal-CT, and clinoptilolite occur in the Upper Cretaceous Winning Group onshore. Similar Upper Cretaceous altered vitric ash occurs in hole 249 of the Deep-Sea Drilling Project (*14*) near the east coast of South Africa.

Opal-CT silicifications associated with smectite-dominated clay assemblages and accompanied by clinoptilolite, glauconite, and sponge spicules occur in Cretaceous sediments of southern England from the Aptian on, and similar assemblages occur in the Gulf states of the United States. It has been suggested that both are the result of volcanic activity associated with the separation of Europe and America starting in Aptian-Albian times (*15*). Thus the trailing margins of continents bounding the Atlantic, Indian, and Southern Oceans are characterized by the occurrence of explosive volcanism soon after or contemporaneous with the onset of various phases of rifting. Williams and Corliss (*16*) have emphasized other geological similarities between the continental margins of southern Australia and the eastern United States. Pacey (*17*) suggested that the magma responsible for the extensive post Cenomanian British deposits was pantelleritic with the explosive volcanism related to the final separation of Greenland and northwestern Europe. Since separation of Australia from Antarctica has also produced explosive, silicic volcanism it seems likely that other such margins are so characterized. The presence of abundant clinoptilolite (*18*) and opal-CT may allow recognition of these margins and provide a useful means of interpreting older parts of the geologic record.

J. B. JONES
M. J. FITZGERALD
Department of Geology and Mineralogy, University of Adelaide, Adelaide, South Australia 5001

References and Notes

1. M. A. Reynolds, *Trans. R. Soc. South Aust.* **76**, 114 (1953).
2. For details of the lithostratigraphy, see R. J. F. Jenkins, J. B. Jones, B. McGowran, A. S. Beecroft, M. J. Fitzgerald, *Q. Geol. Notes Geol. Surv. South Aust.* **84**, 2 (1984).
3. The method of R. C. Reynolds and J. Hower [*Clays Clay Min.* **18**, 25 (1970)] was used.
4. T. L. Vallier and R. B. Kidd, in *Indian Ocean Geology and Biostratigraphy*, J. R. Heitzler, H. M. Bolli, T. A. Davies, J. B. Saunders, J. G. Slater, Eds. (American Geophysical Union, Washington, D.C., 1977), pp. 87–118.
5. J. R. Hein and D. W. Scholl, *Geol. Soc. Am. Bull.* **89**, 197 (1978).
6. This should not be confused with the Plantagenet Formation of the North Atlantic [L. F. Jansa, P. Enas, B. E. Lucholke, F. M. Gradstein, R. E. Sheridan, in *Deep Drilling Results in the Atlantic Ocean: Continental Margins and Paleoenvironment*, M. Talwari, W. Hay, W. B.

F. Ryan, Eds. (Maurice Ewing Series, American Geophysical Union, Washington, D.C., 1979), vol. 3, pp. 1–57]. The formal definition of the Plantagenet Group precedes this by more than a decade [A. E. Cockbain, *Western Aust. Geol. Surv. Annu. Rep. 1967* (1968), pp. 61–63].
7. A. Beecroft and B. McGowran, personal communication.
8. W. J. Stuart, thesis, University of Adelaide, South Australia (1969).
9. N. H. Ludbrook, in *Handbook of South Australian Geology*, L. W. Parkin, Ed. (Geological Survey, Adelaide, South Australia 1969), pp. 172–203.
10. C. Abele, P. R. Kenley, G. Holdgate, D. Ripper, in *Geology of Victoria*, J. G. Douglas and J. A. Ferguson, Eds. (Geological Society, Melbourne, Australia, 1976), pp. 177–274.
11. B. J. Cooper, *Rep. Invest. Geol. Surv. S. Aust. 50* (1979).
12. D. E. Hayes *et al.*, *Init. Rep. Deep-Sea Drill. Proj.* **28** (1975).
13. J. P. Kennett *et al.*, *ibid.* **29** (1974).
14. E. S. W. Simpson *et al.*, *ibid.* **25** (1974).
15. C. V. Jeans, R. J. Merriman, J. G. Mitchell, D. J. Bland, *Clay Min.* **17**, 105 (1982).
16. D. F. Williams and B. H. Corliss, in *The Ocean Basins and Margins*, A. E. M. Nairn and F. G. Stehli, Eds. (Plenum, New York, 1982), pp. 545–579.
17. N. R. Pacey, *Earth Planet. Sci. Lett.* **67**, 48 (1984).
18. R. L. Hay, *Geol. Soc. Am. Spec. Pap. 85* (1966).
19. We thank A. F. Trendall for specimens from the Plantagenet Group. We also thank A. Beecroft, and V. A. Gostin, R. J. F. Jenkins, and B. McGowran for helpful discussions, several anonymous referees much for their suggestions, and S. Proferes for drafting the figure. The photographs were taken on an Etec Autoscan in University of Adelaide Electron Optical Centre. Supported by ARGS grant E7815352 and forms part of IGCP Project 187, Siliceous Deposits of the Pacific and Tethys Regions.

28 February 1984; accepted 1 August 1984

Chromosomal Location of Human T-Cell Receptor Gene $T_i\beta$

Abstract. *A complementary DNA probe corresponding to the β-chain gene of T_i, the human T lymphocyte receptor, has been molecularly cloned. The chromosomal origin of the $T_i\beta$ gene was determined with the complementary DNA by screening a series of 12 cell hybrid (mouse × human) DNA's containing overlapping subsets of human chromosomes. DNA hybridization (Southern) experiments showed that the human $T_i\beta$ gene resides on chromosome 7 and is thus not linked to the immunoglobulin loci or to the major histocompatibility locus in humans.*

Studies of both human and murine systems have shown that the receptor for antigen and major histocompatibility complex on T lymphocytes belongs to a novel class of 80- to 90-kilodalton (kD) disulfide-linked heterodimer that expresses clonotypic epitopes (*1–5*). In humans, these molecules—termed T_i—are each comprised of one 49- to 51-kD α subunit and one 43-kD β subunit that are, in turn, noncovalently associated with the invariant 20- and 25-kD T3 molecules (*6*). Recently, amino-terminal amino acid sequencing and molecular cloning techniques have identified the $T_i\beta$ gene and shown that it has a distant but definite homology with immunoglobulin light chains (*3, 6–9*). The availability of complementary DNA (cDNA) probes for the $T_i\beta$ genomic sequence (*7*) makes it possible to ascertain its chromosomal position.

We constructed a genetic mapping panel of hybrids of mouse × human somatic cells that contain overlapping subsets of human chromosomes on a rodent genetic background. In effect, the panel served to isolate small groups of human chromosomes that could be screened for the presence of the $T_i\beta$ gene by nucleic acid homology with the corresponding cDNA probe. The distribution of human chromosomes across the panel was determined by isoenzyme and karyotype analysis (*10*) and in certain cases by human DNA probes whose map location has been established. The distribution of $T_i\beta$ genomic sequences across the panel was independently determined by molecular hybridization of cell hybrid DNA with an isotopically labeled $T_i\beta$ cDNA probe (*7, 11*). Comparison of the two sets of data enabled assignment of any hybridization band to a specific human chromosome. Further, segregation of various $T_i\beta$-specific bands with respect to each other gave an indication of genetic linkage among bands. This approach therefore allowed chromosomal assignment of the structural gene as well as unlinked but related human $T_i\beta$-like DNA sequences. Samples of human, mouse, or mouse × human cell hybrid genomic DNA's (20 μg each) were cleaved with restriction endonuclease Eco RI, separated by agarose gel electrophoresis, transferred to nitrocellulose, and probed with the pβREX plasmid for the $T_i\beta$ gene (*7*) (Fig. 1). Genomic mouse A9 DNA cleaved with Eco RI (lanes c and k) showed a single intense 2.3-kilobase (kb) Eco RI band. In addition, two very large, less intense bands representing mouse DNA were observed, both greater than 9.5-kb. Under these conditions, their sizes could not be accurately determined. Human HeLa DNA cleaved with Eco RI (lanes d and l) contained four intensely hybridizing bands with apparent sizes of 2.0, 5.2, and 7.0 kb and a very large band in excess of 9.5 kb. These results indicate that somatic cell hybrid DNA's cleaved with Eco RI and probed with isotopically labeled pβREX should each contain mouse DNA–specific bands corresponding to the mouse A9 DNA genetic background. In addition, those hybrid cell DNA's that contain the chromosome bearing the human $T_i\beta$ gene should contain human DNA–specific Eco RI bands.

Twelve hybrid (mouse × human) somatic cell DNA's were screened by Southern blotting (*12*) for the presence of human $T_i\beta$ DNA sequences. As predicted, each cell hybrid DNA (Fig. 1, lanes e to j and m to r) contained the 2.3-kb mouse DNA–specific $T_i\beta$ band. Two hybrids, FRY4.A+SEG and 53-87(3)cl.10 (Fig. 1, lanes h and j, respectively), showed all three human DNA–specific $T_i\beta$ bands between 2.0 and 7.0 kb. The large band representing human $T_i\beta$ DNA also appeared to be present in these two hybrid DNA's; however, mouse DNA–specific bands migrating together with this band obscured the analysis. A third somatic cell hybrid DNA, BDA 14b25

Table 1. Chromosomal content of somatic cell hybrid cell lines assayed by cytogenetic and isoenzyme analysis (*10, 15, 22*). Chromosomes listed include translocation chromosomes present.

Hybrid cell DNA	Human chromosomes present	Blot hybridization result with pβREX
BDA 10a3	2,3,5,6,8,9,10,11,13,14,16,17,20,22,X	−
BDA 10a4aF9-1	2,4,5,6,8,12,14,X	−
BDA 17b17	1,3,4,5,9,12,14,15,18,19,20,21,22,X	−
FRY 4.A+SEG	1,2,3,4,6,7,8,10,11,12,14,15,18,21,22,X	+
BDA 14b25	1,2,3,4,7,12,14,15,X	+*
53-87(3)cl.10	7	+
AHA 16e	10,11,12,13,14,17,18,19,20,21,X	−
AHA 3d2-2	1,4,15	−
AHA 3d2-3	3,4,8,11,12,18,19	−
AHA 16e-3	1,3,4,10,11,12,13,19,21,X	−
AHA 16e-6	1,2,3,4,10,11,13,14,16,19,20,X	−
41pT2A	1,3,4,8,10,12,14,15,16,18,19,21,X	−

*Weak positive hybridization.